01 Jul 1994

A Magnetic, Neutron Diffraction, and Mössbauer Spectral Study of $Nd_2Fe_{15}Ga_2$ and the $Tb_2Fe_{17-x}Ga_x$ Solid Solutions

Zhong Bo Hu

William B. Yelon
Missouri University of Science and Technology

Sanjay R. Mishra

Gary J. Long
Missouri University of Science and Technology, glong@mst.edu

et. al. For a complete list of authors, see https://scholarsmine.mst.edu/phys_facwork/178

Recommended Citation

Z. B. Hu et al., "A Magnetic, Neutron Diffraction, and Mössbauer Spectral Study of $Nd_2Fe_{15}Ga_2$ and the $Tb_2Fe_{17-x}Ga_x$ Solid Solutions," *Journal of Applied Physics*, vol. 76, no. 1, pp. 443-450, American Institute of Physics (AIP) Publishing, Jul 1994.
The definitive version is available at https://doi.org/10.1063/1.357094

A magnetic, neutron diffraction, and Mössbauer spectral study of $Nd_2Fe_{15}Ga_2$ and the $Tb_2Fe_{17-x}Ga_x$ solid solutions

Z. Hu and W. B. Yelon
University of Missouri Research Reactor and the Departments of Chemistry and Physics, University of Missouri-Columbia, Columbia, Missouri 65211

S. Mishra, Gary J. Long, and O. A. Pringle
Departments of Chemistry and Physics, University of Missouri-Rolla, Rolla, Missouri 65401-0249

D. P. Middleton and K. H. J. Buschow
Philips Research Laboratories, P.O. Box 80000, NL-5600 JA Eindhoven, The Netherlands

F. Grandjean
Institute of Physics, B5, University of Liège, B-4000 Sart-Tilman, Belgium

(Received 10 December 1993; accepted for publication 19 March 1994)

An x-ray diffraction study of the substitution of gallium in Tb_2Fe_{17} to form the $Tb_2Fe_{17-x}Ga_x$ solid solutions indicates that the compounds adopt the rhombohedral Th_2Zn_{17} structure. The unit cell volume and the a-axis lattice parameter increase linearly with increasing gallium content. The c-axis lattice parameter increases linearly from $x=0$ to 6 and then decreases between $x=7$ and 8. Magnetic studies show the Curie temperature increases by ~150° above that of Tb_2Fe_{17} to reach a maximum between $x=3$ and 4, and then decreases with further increases in x. Neutron diffraction studies of $Nd_2Fe_{15}Ga_2$ and $Tb_2Fe_{17-x}Ga_x$, with x equal to 5, 6, and 8, indicate that the gallium completely avoids the $9d$ site, occupies the $6c$ "dumbell" site only at high values of x and strongly prefers the $18f$ site at high values of x. The magnetic neutron scattering indicates both that the terbium sublattice magnetization couples antiferromagnetically with the iron sublattice and that there is a change in easy magnetization direction from planar to axial with increasing gallium concentration. This change in easy magnetization direction is explained in terms of a sign reversal of the second-order crystal field parameter, A_2^0, the most important parameter responsible for determining the terbium sublattice anisotropy. The Mössbauer effect spectra indicate a larger room-temperature average hyperfine field at the iron site in the $Tb_2Fe_{17-x}Ga_x$ solid solutions than in several related R_2Fe_{17} compounds. The large observed increase in the isomer shift with increasing gallium content results from interatomic charge transfer and intraatomic s-d charge redistribution in the presence of gallium.

I. INTRODUCTION

The discovery[1,2] of the good permanent magnet properties of modified iron-based rare-earth transition-metal intermetallic compounds has stimulated renewed research in this field. The interstitially modified $Sm_2Fe_{17}C_x$, $Sm_2Fe_{17}N_x$, and $NdFe_{11}TMN_x$ compounds all have high-energy products at room temperature and Curie temperatures high enough to make them useful in a wide variety of magnetic applications. An important feature distinguishes these compounds from their analogous binary compounds, all of which are unsuitable for magnetic applications because of their low Curie temperatures. In the interstitial compounds, the iron-iron distances are increased as compared to those found in the binary compounds, an increase which substantially increases their Curie temperatures. Unfortunately, although these interstitial compounds appear to be promising hard permanent magnetic materials, they are thermodynamically unstable and decompose into rare-earth nitrides and α iron at high temperatures. Thus, the processing of these interstitial compounds, for instance by sintering, is difficult. An alternative route to increased bond distances, and hence Curie temperatures, is to force the lattice to expand by replacing some of the iron by an element with a larger metallic radius. Although the iron moments may be diluted by this replacement, the possibility of producing useful hard permanent magnets is, nevertheless, worth pursuing.

We have previously reported[3] that aluminum substitution in Nd_2Fe_{17} to produce the $Nd_2Fe_{17-x}Al_x$ solid solutions, leads to an increased Curie temperature for values of x of less than ~5. The maximum in the Curie temperature occurs at $x=3.5$. In these solid solutions, the unit cell volume increases by ~9 Å^3 per aluminum atom. Silicon substitution[4] also leads to an enhancement of the Curie temperature, although in this case the lattice actually contracts slightly. The mechanism for this enhancement is currently under investigation. In view of the beneficial effect of silicon and aluminum substitution in Nd_2Fe_{17}, gallium substitution is an obvious choice for further study. Herein we report the results of a magnetic, neutron diffraction, and Mössbauer effect study of $Nd_2Fe_{15}Ga_2$, and several $Tb_2Fe_{17-x}Ga_x$ solid solutions.

II. EXPERIMENT

The samples were prepared from 99.9% pure elements by arc melting. The samples were then annealed at 1050 °C for three weeks and their phase purity was checked by x-ray diffraction with Cu K_α radiation on a Philips PW 1800/10 x-ray diffractometer equipped with a single-crystal graphite

 0021-8979/94/76(1)/443/8/$6.00

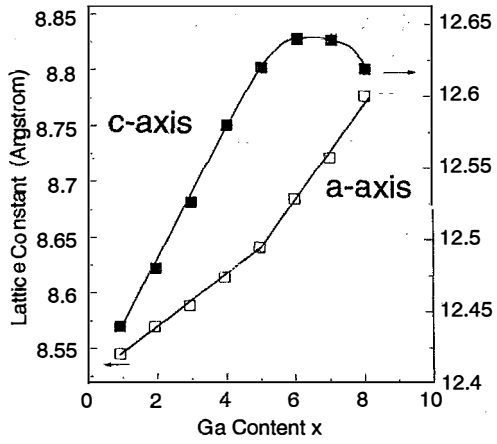

FIG. 1. The room-temperature lattice constants of the rhombohedral $Tb_2Fe_{17-x}Ga_x$ solid solutions as a function of gallium content.

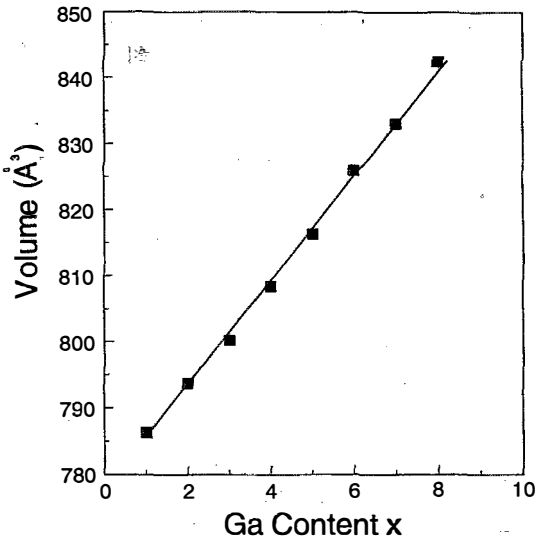

FIG. 3. The room-temperature unit cell volume of the rhombohedral $Tb_2Fe_{17-x}Ga_x$ solid solutions as a function of gallium content.

monochromator. X-ray diffraction results indicate that $Nd_2Fe_{17-x}Ga_x$ will form single-phase solid solutions only for x values up to ~2. Unfortunately, for x values less than ~1, the $Tb_2Fe_{17-x}Ga_x$ solid solutions crystallize in the hexagonal Th_2Ni_{17} structure and, as a result, may be nonstoichiometric and possess a considerable degree of disorder, a complication which has been reported previously.[5] However, samples of $Tb_2Fe_{17-x}Ga_x$, with x values greater than ~1, annealed at 1050 °C for three weeks and quenched in water crystallize in the rhombohedral Th_2Zn_{17} structure, a structure which has consistently been found to be stoichiometric and free from disorder. Neutron diffraction studies of the $Tb_2Fe_{17-x}Ga_x$ solid solutions were restricted to samples with x values above 3.

The magnetic properties of the free particle samples were measured on a superconducting quantum interference device (SQUID) magnetometer between 5 and 300 K and on a Faraday magnetometer between 300 and 1000 K. The Curie temperatures were determined in small magnetic fields of ~0.05 T by plotting the square of the magnetization versus temperature and extrapolating the steepest part of the curve to zero magnetization.

The powder neutron diffraction patterns were collected at the University of Missouri Research Reactor by using a linear position sensitive diffractometer and neutrons with a wavelength of 1.4783 Å. The data for each sample were collected over ~24 h at room temperature between 2θ angles of 5° and 105° on ~2 g of finely powdered sample placed in a thin wall vanadium container. Refinements of the neutron diffraction data were carried out with the FULLPROF computer code which permits multiple phase refinement as well as magnetic structure refinement of each of the coexisting phases. $Nd_2Fe_{15}Ga_2$ was found to contain ~3% by volume of

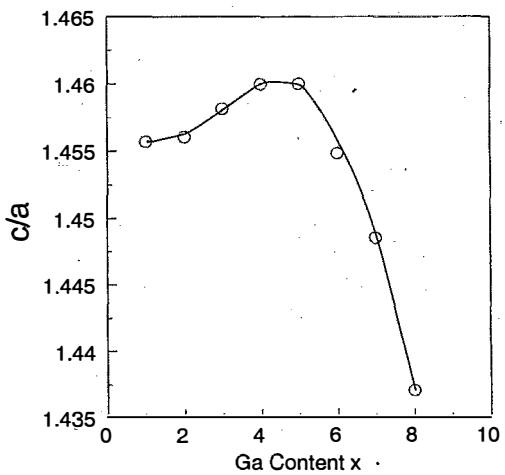

FIG. 2. The room-temperature c/a lattice parameter ratio of the rhombohedral $Tb_2Fe_{17-x}Ga_x$ solid solutions as a function of gallium content.

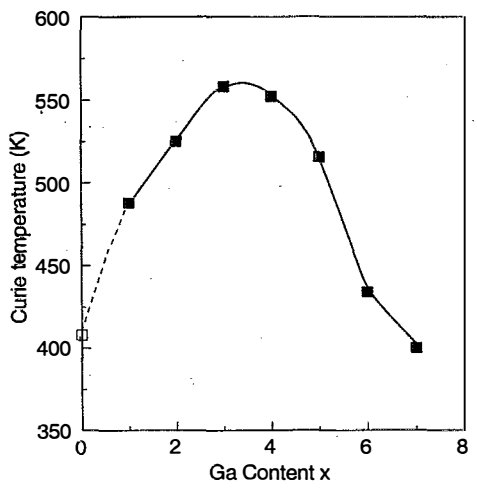

FIG. 4. The Curie temperature of the rhombohedral $Tb_2Fe_{17-x}Ga_x$ solid solutions as a function of gallium content. The open symbol is the Curie temperature of hexagonal Tb_2Fe_{17}, obtained from Ref. 11.

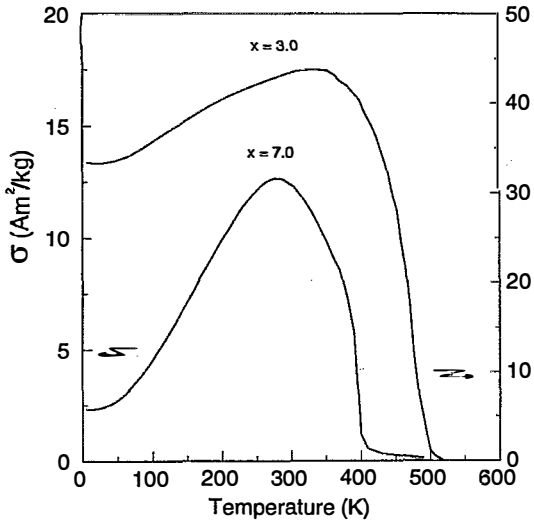

FIG. 5. The temperature dependence of the magnetization of $Tb_2Fe_{17-x}Ga_x$ obtained in an applied field of 10 kOe for $x=3$ and 0.5 kOe for $x=7$.

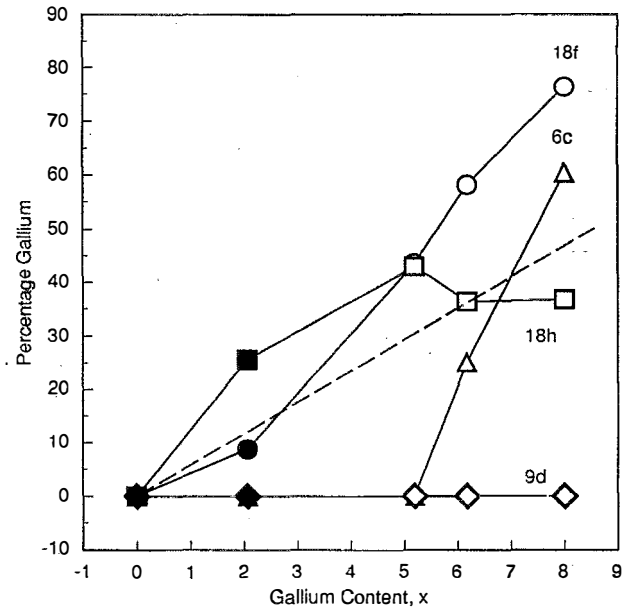

FIG. 6. The percentage gallium found on the four crystallographic iron sites in Nd_2Fe_{17}, $Nd_2Fe_{15}Ga_2$, closed symbols, and the $Tb_2Fe_{17-x}Ga_x$ solid solutions, open symbols, as a function of gallium content. The dashed line represents random occupancy by gallium.

α-iron whereas $Tb_2Fe_{17-x}Ga_x$, where x is 5, 6, and 8, were found to be essentially pure rhombohedral phase solid solutions.

The Mössbauer spectra were obtained at the University of Missouri-Rolla at several temperatures on a Harwell constant-acceleration spectrometer which utilized a room-temperature rhodium matrix cobalt-57 source and was calibrated at room temperature with α-iron foil. The Mössbauer absorbers, which were ~30 mg/cm^2 thick, were prepared from powdered samples which had been sieved to a 0.045 mm or smaller particle diameter. The resulting spectra have been fit as discussed below and elsewhere[6] and the estimated

TABLE I. The room-temperature lattice and positional parameters, site occupancies, and moments in $Nd_2Fe_{15}Ga_2$ and $Tb_2Fe_{17-x}Ga_x$ as measured by neutron diffraction.

Compound	$Nd_2Fe_{15}Ga_2$	$Tb_2Fe_{12}Ga_5$	$Tb_2Fe_{11}Ga_6$	$Tb_2Fe_9Ga_8$
x	2.064	5.196	6.180	8.004
a, Å	8.628(1)	8.6371(1)	8.6750(2)	8.7669(2)
c, Å	12.5531(2)	12.6091(2)	12.6240(3)	12.6045(4)
V, Å^3	809.30	814.62	822.74	838.97
Nd or Tb, 6c, z	0.3415(3)	0.3411(3)	0.3426(3)	0.3510(4)
Fe/Ga, 6c, z	0.0957(2)	0.0973(2)	0.0996(3)	0.1113(5)
Fe/Ga, 18f, x	0.2885(1)	0.2904(1)	0.2922(2)	0.3067(3)
Fe/Ga, 18h, x	0.1692(1)	0.1690(1)	0.1685(1)	0.1668(2)
Fe/Ga, 18h, z	0.4891(1)	0.4882(1)	0.4884(1)	0.4898(2)
%Ga, 6c	0.0	0.0	25.15	60.47
%Ga, 9d	0.0	0.0	0.0	0.0
%Ga, 18f	8.8	43.6	58.2	76.4
%Ga, 18h	25.6	43.0	36.4	36.8
R factor	4.91	5.41	6.59	6.63
R_w factor	6.63	7.33	8.68	8.79
R_m factor	3.84	5.98	9.33	8.63
χ^2	3.34	3.61	4.51	4.66
μ, Nd or Tb, 6c, μ_B	1.8(2)[a]	−4.5(1)[a]	−4.6(1)[b]	−4.1(1)[b]
μ, Fe, 6c, μ_B	2.9(2)[a]	2.7(1)[a]	1.8(1)[b]	1.6(3)[b]
μ, Fe, 9d, μ_B	2.0(1)[a]	1.8(1)[a]	1.3(1)[b]	1.2(1)[b]
μ, Fe, 18f, μ_B	2.1(2)[a]	2.2(1)[a]	2.1(2)[b]	1.5(3)[b]
μ, Fe, 18h, μ_B	1.6(3)[a]	1.3(1)[a]	1.3(1)[b]	1.2(1)[b]
μ cell, μ_B	102.60	42.63	22.83	9.98
μ formula, μ_B	34.20	14.21	7.61	3.33
α-Fe, vol %	3.47	0.0	0.0	0.0

[a]The magnetic moments are oriented along [100].
[b]The magnetic moments are oriented along [001].

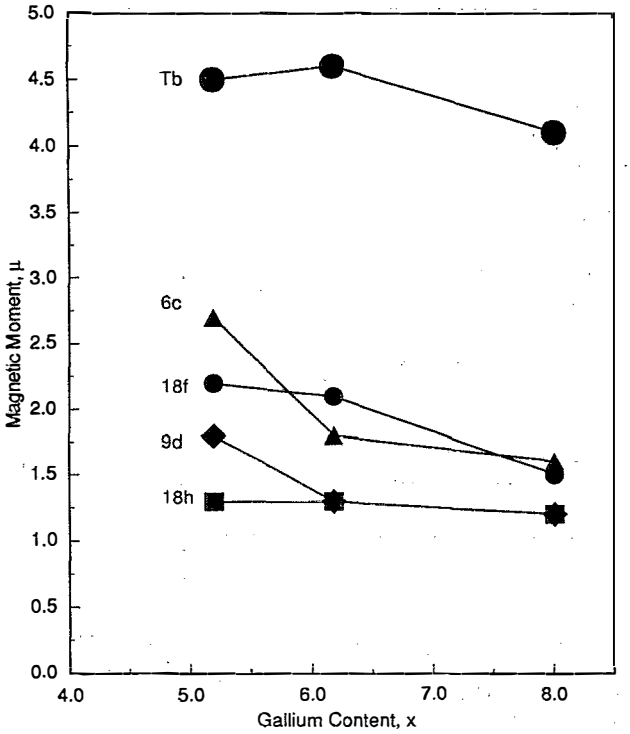

FIG. 7. The magnetic moments found for the different crystallographic sites in the $Tb_2Fe_{17-x}Ga_x$ solid solutions as a function of gallium content.

errors are ±1 kOe for the weighted average hyperfine fields and ±0.005 mm/s for the weighted average isomer shifts.

III. RESULTS

X-ray diffraction results for the $Tb_2Fe_{17-x}Ga_x$ solid solutions indicate that their lattice parameters change dramatically with increasing gallium content. As shown in Fig. 1, the *c*-axis lattice parameter increases almost linearly from $x=1$ to 5 with a slope of 0.045 Å/Ga, remains constant at $x=5$, 6, and 7, and then decreases slightly at $x=8$. In contrast, the *a*-axis lattice parameter increases monotonically and almost linearly with increasing gallium content with a slope of 0.034 Å/Ga. This behavior is rather different than that found[3] for the $Nd_2Fe_{17-x}Al_x$ solid solutions in which both lattice parameters increase nearly linearly from $x=0$ to 9 with a slope of 0.045 Å/Al for the *c* axis and 0.032 Å/Al for the *a* axis.

As a result of the differing compositional dependencies of the lattice parameters, the *c*/*a* ratio shows a maximum at $Tb_2Fe_{13}Ga_4$, as is shown in Fig. 2, a maximum which is very similar to that found[3] in $Nd_2Fe_{17-x}Al_x$. Surprisingly, as is shown in Fig. 3, the unit cell volume shows a virtually linear increase of 8.3% or 8 Å^3/Ga between the calculated value of 766.2 Å^3 for the rhombohedral unit cell of Tb_2Fe_{17} and the value obtained for $Tb_2Fe_9Ga_8$. These increases are only slightly smaller than the increase of 9.4% or 9 Å^3/Al found[3] between Nd_2Fe_{17} and $Nd_2Fe_9Al_8$. It should be noted that in both series of solid solutions the increases are larger than the 6.8% and 6.6% increase in the unit cell volume of Pr_2Fe_{17} and Nd_2Fe_{17} upon nitrogenation.[7–9]

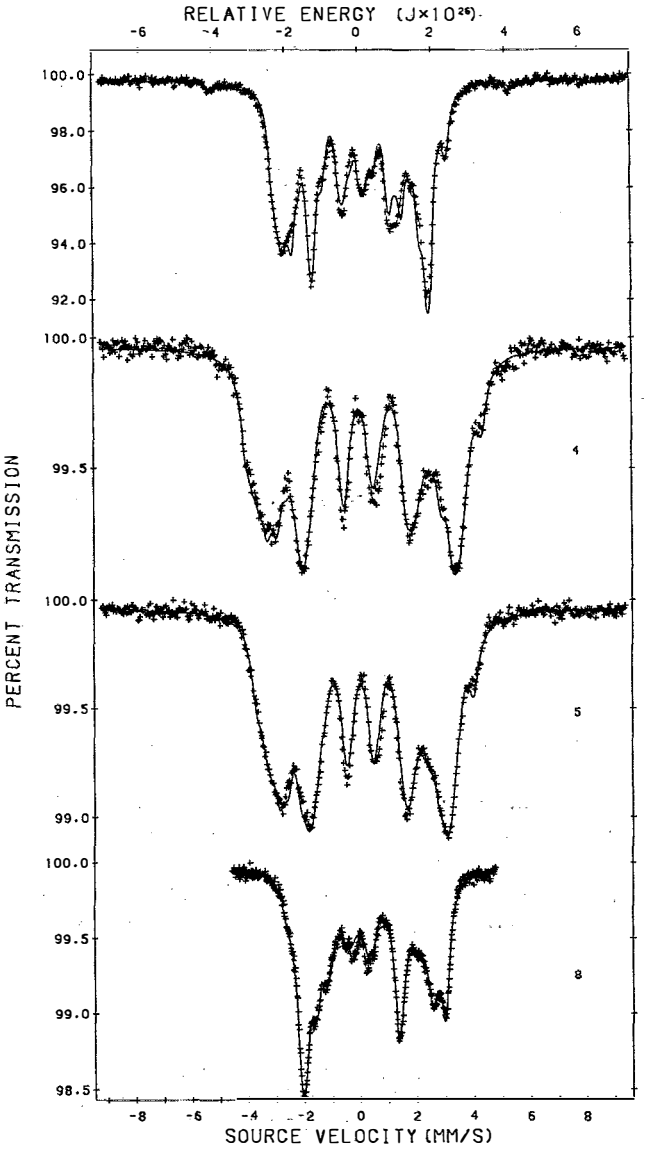

FIG. 8. The Mössbauer spectra of Nd_2Fe_{17}, top, and the $Tb_2Fe_{17-x}Ga_x$ solid solutions obtained at 295 K.

The variation of the Curie temperature with gallium content is shown in Fig. 4, which reveals a maximum in the Curie temperature between $Tb_2Fe_{14}Ga_3$ and $Tb_2Fe_{13}Ga_4$. A similar maximum has been observed[3,10] in $Y_2Fe_{17-x}Al_x$, $Nd_2Fe_{17-x}Al_x$, and $Ho_2Fe_{17-x}Al_x$. This figure also reveals that the Curie temperatures of all the $Tb_2Fe_{17-x}Ga_x$ solid solutions, except for $Tb_2Fe_{10}Ga_7$, are higher than that reported[11,12] for hexagonal Tb_2Fe_{17}, which is shown as the open square in Fig. 4. The temperature dependence of the magnetization of $Tb_2Fe_{14}Ga_3$ and $Tb_2Fe_{10}Ga_7$ is shown in Fig. 5. The maximum in the magnetization occurs at ~340 K for $Tb_2Fe_{14}Ga_3$ and ~290 K for $Tb_2Fe_{10}Ga_7$. Below these temperatures the magnetization falls, indicating antiferromagnetic coupling of the terbium sublattice magnetization with that of the iron sublattices.

TABLE II. Weighted average isomer shifts and hyperfine fields in $Tb_2Fe_{17-x}Ga_x$.

Compound	Isomer shift[a] (mm/s)		Hyperfine field (kOe)	
	85 K	295 K	85 K	295 K
Pr_2Fe_{17}[b]	0.049	−0.092	286	0
Nd_2Fe_{17}[c]	0.061	−0.071	292	157
Tb_2Fe_{17}	0.034	−0.114	307	229
$Tb_2Fe_{16}Ga$	0.045	−0.065	292	239
$Tb_2Fe_{15}Ga_2$	0.075	−0.039	274	235
$Tb_2Fe_{14}Ga_3$	0.114	−0.012	259	226
$Tb_2Fe_{13}Ga_4$	0.138	0.024	240	209
$Tb_2Fe_{12}Ga_5$	0.192	0.070	224	190
$Tb_2Fe_{11}Ga_6$	0.240	0.130	202	163
$Tb_2Fe_9Ga_8$	0.313	0.212	174	148

[a]Relative to room temperature natural abundance α iron.
[b]Data obtained from Ref. 7.
[c]Data obtained from Ref. 13.

The results of the refinement of the powder neutron diffraction patterns for the four samples studied are given in Table I. The neutron diffraction derived unit cell lattice parameters for the $Tb_2Fe_{17-x}Ga_x$ solid solutions agree very well with those measured by x-ray diffraction and shown in Fig. 1. The total gallium content in the $Tb_2Fe_{17-x}Ga_x$ solid solutions, as calculated from the refined fractional occupancies, is in good agreement with the nominal gallium content. The gallium is found only on the transition metal sites and the percentage gallium found on each of the four iron sites is shown as a function of gallium content in Fig. 6. Previous studies on a wide variety of rare-earth–transition-metal intermetallic compounds have shown that the preferred occupancy of the transition metal is independent of the rare earth, and thus it is appropriate to show the results for $Nd_2Fe_{15}Ga_2$ and the $Tb_2Fe_{17-x}Ga_x$ solid solutions on the same plot.

The pattern of replacement of iron by gallium is similar to that observed[3] with aluminum. Because both aluminum and gallium have larger metallic radii than iron, they avoid, for all x values studied, the iron $9d$ site, the site which has the smallest Wigner–Seitz cell volume.[7,13,14] The $6c$ site has the largest Wigner–Seitz cell volume and hence it is surprising that gallium does not occupy this site in $Tb_2Fe_{12}Ga_5$. In contrast aluminum occupies[3] the $6c$ site even at lower aluminum concentrations in $Nd_2Fe_{17-x}Al_x$. The occupancy by gallium or aluminum of the $18h$ site, which has next to the largest Wigner–Seitz cell volume, is similar and virtually constant above $x=5$ in $Tb_2Fe_{17-x}Ga_x$ and above $x=4$ in $Nd_2Fe_{17-x}Al_x$. In contrast, the $18f$ site takes up more gallium than aluminum such that, in the $Tb_2Fe_{17-x}Ga_x$ solid solutions, the $18f$ site contains up to ~75% gallium. Once a specific site is occupied by aluminum or gallium, its near neighbors are less likely, because of crowding, to accept aluminum or gallium. Alternatively, if a site is unoccupied by aluminum or gallium, as is the case for the $9d$ site, then its near neighbors are more likely to accept aluminum or gallium. Thus, because the $9d$ site has four $18f$ and four $18h$ near neighbors, these latter sites are more likely to accept aluminum or gallium, accounting, at least in part, for the higher aluminum or gallium occupancy of these sites. Unfor-

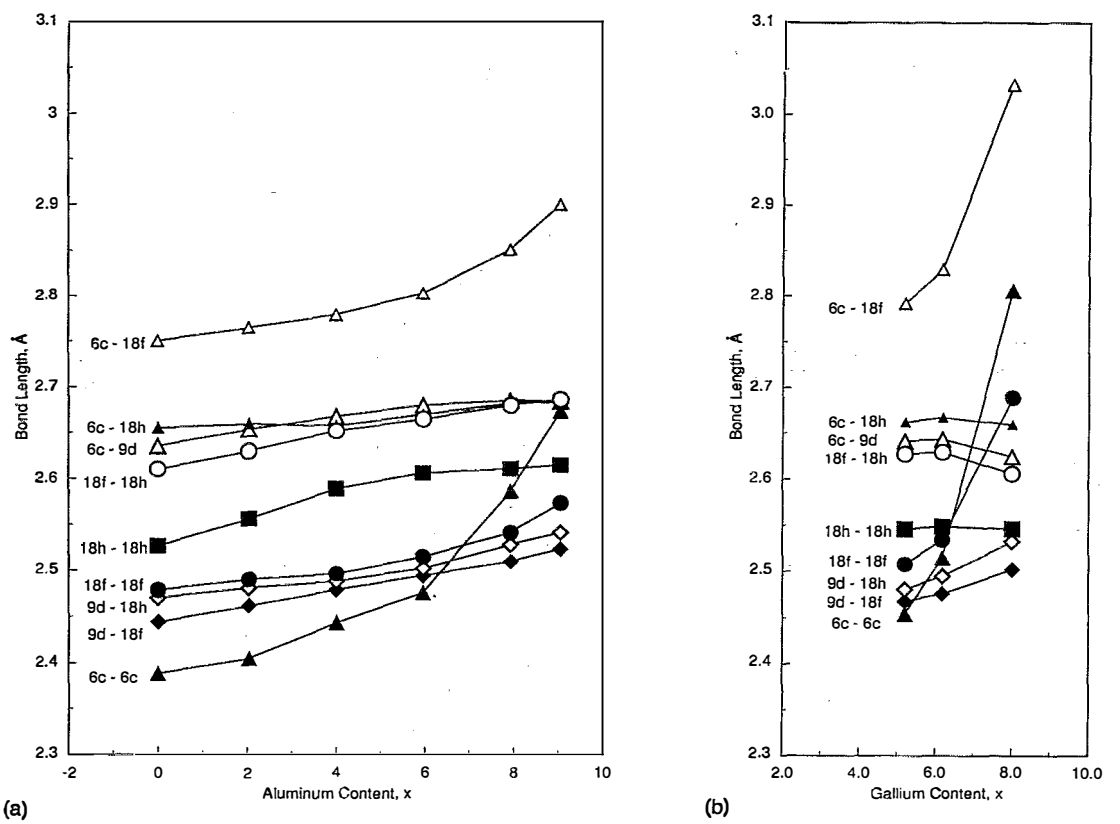

FIG. 9. The bond lengths as a function of aluminum content in $Nd_2Fe_{17-x}Al_x$ (A) and as a function of gallium content in $Tb_2Fe_{17-x}Ga_x$ (B).

tunately there seems to be no simple explanation for the added preference of gallium for the $18f$ sites.

The magnetic behavior of the $Tb_2Fe_{17-x}Ga_x$ solid solutions is quite extraordinary. As expected from the variation in the Curie temperature, see Fig. 4, the magnetic moment per formula unit is largest for $Tb_2Fe_{12}Ga_5$ and decreases with increasing gallium content, see Table I. The compositional dependence of the magnetic moments for the different sites in these solid solutions is given in Fig. 7. The individual iron moments decrease somewhat with gallium content but the weighted average moment is still $1.37\mu_B$ for $Tb_2Fe_9Ga_8$. In agreement with the magnetization measurements, see Fig. 5, the terbium sublattice magnetization couples antiferromagnetically with the iron sublattice and carries a magnetic moment of $4.1\mu_B$ at the highest gallium concentration. Unexpectedly, the easy axis of magnetization changes from basal in $Tb_2Fe_{12}Ga_5$ to axial in the higher gallium content solid solutions. A similar change is not observed[15] in the $Nd_2Fe_{17-x}Al_x$ solid solutions. The reasons for these differences will be discussed below.

The Mössbauer effect spectra of the $Tb_2Fe_{17-x}Ga_x$ solid solutions measured at 295 K are shown in Fig. 8. Very similar spectra were observed at 85 K. The spectra of $Tb_2Fe_{13}Ga_4$ and $Tb_2Fe_{12}Ga_5$ were fit with seven sextets corresponding to the seven magnetically inequivalent iron sites expected[7,13] for a basal orientation of the magnetization. The spectra of $Tb_2Fe_9Ga_8$ were fit with four sextets corresponding to the four magnetically inequivalent iron sites expected[14] for an axial orientation of the magnetization. The relative areas of these sextets were constrained to those calculated for iron occupancies on the basis of the gallium occupancies given in Table I. The hyperfine parameters were adjusted to be consistent with those found[7,16,17] for related R_2Fe_{17} compounds. The resulting weighted average hyperfine fields and isomer shifts, δ, are given in Table II and reveal, as expected, that the hyperfine field is largest for $Tb_2Fe_{16}Ga$ and decreases with increasing gallium content. The dramatic influence of gallium on the room-temperature hyperfine field in the $Tb_2Fe_{17-x}Ga_x$ solid solutions is immediately apparent in Table II.

The isomer shifts at 85 and 295 K, given in Table II, increase linearly with increasing gallium content and extrapolate to reasonable values for the isomer shifts of Tb_2Fe_{17}. By using these extrapolated values and that of the unit cell volume of Tb_2Fe_{17}, see Fig. 3, it is possible to calculate values of $\Delta\delta/\Delta \ln V$ for the $Tb_2Fe_{17-x}Ga_x$ solid solutions. The resulting values are 3.8 mm/s at 295 K and 3.2 mm/s at 85 K, both of which are higher than the ~1.0 mm/s value expected[18] for a close packed structure. The high values of $\Delta\delta/\Delta \ln V$ indicate that only approximately one-third of the increase in the isomer shift can be attributed to the lattice expansion. In previous investigations[19,20] it was shown that the isomer shift increases with increasing number of nearest-neighbor gallium atoms as a result of the interatomic charge transfer and intraatomic s-d charge redistribution. The observed isomer shift increases in the $Tb_2Fe_{17-x}Ga_x$ solid solutions can be satisfactorily understood on the same basis.

IV. DISCUSSION

With the exception of the different behavior of the c lattice parameter, the behavior of the crystal lattice upon gallium substitution in Tb_2Fe_{17} is similar to that of aluminum substitution in Nd_2Fe_{17}. In contrast, as shown in Fig. 9, the behavior of the metal-metal bond lengths for the $Nd_2Fe_{17-x}Al_x$ and $Tb_2Fe_{17-x}Ga_x$ solid solutions is quite different. The most striking feature shown in Fig. 9 is the elongation with substitution of the $6c$-$6c$ bond distance, an elongation which is much more pronounced in the case of the gallium solid solutions. The $6c$-$6c$ bond length, the so-called metal-metal "dumbell" length, is the shortest bond in these solid solutions at low values of x. At high aluminum substitution[3] this bond has an intermediate length, whereas at high gallium substitution, it becomes the next to the longest bond and shows the largest overall increase in bond length. This behavior is very different from that observed upon nitrogenation of R_2Fe_{17} in which case the $6c$-$6c$ bond length remains the shortest and shows an increase smaller than the average iron-iron bond length increase. Indeed, in Nd_2Fe_{17}, the $6c$-$6c$ bond length increases[8,9] from 2.389 to 2.411 Å, an increase of less than 1%, whereas the average increase of all iron-iron bond lengths is 1.9%.

Because of its short $6c$-$6c$ bond length, the $6c$ site is generally believed to be responsible for the low Curie temperature of the R_2Fe_{17} compounds. However, Wigner–Seitz cell calculations[7,13] indicate that this site has 13 iron near neighbors consisting of one Fe $6c$, three Fe $9d$, six Fe $18f$, and three Fe $18h$ sites. In Nd_2Fe_{17}, the respective bond lengths are 2.389 Å to Fe $6c$, 2.625 Å to Fe $9d$, 2.741 Å to Fe $18f$, and 2.655 Å to Fe $18h$. With the exception of the bond to $6c$, all of these bond lengths are expected to lead to ferromagnetic exchange interactions. Hence, because of its high coordination by iron and long bond lengths, the $6c$ site is important in determining the magnetic exchange coupling in these compounds. Although the comparison of the neodymium and terbium compounds may be complex, the $Tb_2Fe_{17-x}Ga_x$ solid solutions appear to be magnetically more highly ordered at higher gallium content than the analogous $Nd_2Fe_{17-x}Al_x$ solid solutions, an improvement which may be related to the reduced gallium substitution on the $6c$ site in the $Tb_2Fe_{17-x}Ga_x$ solid solutions as compared to that in $Nd_2Fe_{17-x}Al_x$. Neutron diffraction results clearly indicate that the initial Curie temperature enhancement in $Tb_2Fe_{17-x}Ga_x$ solid solutions is not a result of the removal of iron $6c$ "dumbell" atoms by substitution of gallium onto these sites. Also influential in determining the magnetic exchange may be the changes in bonding of the $18f$ site. The $18f$-$18f$ bond length moves from the group of shorter bonds in the $Nd_2Fe_{17-x}Al_x$ solid solutions, see Fig. 9(A), to the group of longer bonds in the $Tb_2Fe_{17-x}Ga_x$ solid solutions at higher x values, see Fig. 9(B). In contrast, upon nitrogenation of R_2Fe_{17}, the $18f$-$18f$ bond length remains virtually unchanged whereas the $18h$-$18h$ bond length moves[8,9,16] from the group of short bonds in R_2Fe_{17} to the group of long bonds in $R_2Fe_{17}N_x$. Of course, any consideration of the distance of the iron-iron bonding must be weighted by the magnetic dilution of the nonmagnetic gallium or aluminum on the iron sublattice. From this point of view, the $9d$-$18h$ and $18h$-

$18h$ bond lengths are the most important and the differences between the aluminum and gallium substitutions are less apparent.

It is interesting to compare the effect of gallium substitution versus nitrogenation on the Curie temperature of Tb_2Fe_{17}. The increase[10] in Curie temperature upon nitrogenation is ~320°. In the $Tb_2Fe_{17-x}Ga_x$ solid solutions, an increase of 150° between Tb_2Fe_{17} and $Tb_2Fe_{14}Ga_3$ is observed, see Fig. 4. This increase is of course smaller because of the magnetic dilution by diamagnetic gallium. Thus it would seem that the origin of the increase in Curie temperature is different in the $Tb_2Fe_{17-x}Ga_x$ solid solutions and in the nitrided compounds.

Of particular interest is the change in the easy axis of magnetization from basal to axial with increasing gallium concentration, a change which requires more detailed discussion. To a first approximation, the total magnetocrystalline anisotropy constant is the sum of the first-order anisotropy constants of the rare earth, R, and iron sublattices,

$$K_1[\text{total}]=K_1[\text{Fe}]+K_1[\text{R}]. \tag{1}$$

It is well known[2] that K_1[Fe] is negative for the R_2Fe_{17} compounds. Indeed this negative value is one of the reasons why the R_2Fe_{17} compounds are not suitable permanent magnet materials. At room temperature the rare-earth sublattice anisotropy is too small to overcome the iron easy plane anisotropy. The rare-earth sublattice anisotropy can be expressed[21] in crystal field terms as

$$K_1[\text{R}]=-(3/2)\alpha_J\langle r_{4f}^2\rangle\langle 3J_z^2-J(J+1)\rangle A_2^0, \tag{2}$$

where α_J is the second-order Stevens factor, the quantities in brackets are expectation values, and A_2^0 is the second-order crystal field parameter, a parameter which is determined predominantly by the rare-earth valence electron charge asphericity.[22,23] A_2^0 is strongly influenced by the variation of x in $R_2Fe_{17-x}Ga_x$, because of the hybridization of the rare-earth $5d$ and $6p$ valence electrons with the valence electrons of its neighboring atoms. Thus, substantial changes in the magnitude and sign of the terbium valence electron asphericity are expected when gallium preferentially substitutes on specific crystallographic sites in the $Tb_2Fe_{17-x}Ga_x$ solid solutions, a preferential substitution which is observed by neutron diffraction, see Fig. 6.

Previous investigations have shown that A_2^0 is small and negative in the rhombohedral R_2Fe_{17} compounds. Because α_J is negative[23] for terbium(III), K_1[Tb] is negative and K_1[Fe] and K_1[Tb] reinforce each other and produce a more negative total anisotropy constant, K_1[total]. The uniaxial orientation of the magnetization in $Tb_2Fe_{11}Ga_6$ indicates that K_1[total] is positive, probably because A_2^0 and thus K_1[Tb] have changed from negative to positive between $Tb_2Fe_{12}Ga_5$ and $Tb_2Fe_{11}Ga_6$.

The A_2^0 parameter may be viewed as an electric field gradient at the rare-earth $4f$ electron which is produced by the terbium valence electron asphericities. A similar, but not identical, electric field gradient is present at the rare-earth nucleus and can be observed as the quadrupole interaction in rare-earth Mössbauer spectroscopy. Thus it is interesting to note that Gd-155 Mössbauer spectra[24] of $Gd_2Fe_{17-x}Al_x$ show a reversal in the sign of the electric field gradient at gadolinium with increasing x. Hence a reversal in the sign of A_2^0 is observed and supports our proposed reason for the change in the easy magnetization direction in $Tb_2Fe_{17-x}Ga_x$ with increasing x. Similar changes could occur with decreasing temperature and low-temperature neutron diffraction studies will be undertaken in the near future to determine whether this occurs in these solid solutions. Finally, a similar change in A_2^0 is no doubt present in the $Nd_2Fe_{17-x}Al_x$ solid solutions.[3] However, the factors preceding A_2^0 in Eq. (2) are considerably smaller for neodymium(III) than for terbium(III) and, as a result, the positive value of K_1[Nd] may not be large enough to compensate the negative value of K_1[Fe].

ACKNOWLEDGMENTS

The authors acknowledge, NATO with thanks, for a cooperative scientific research grant (92-1160), and the Division of Materials Research of the US National Science Foundation, for Grant No. DMR-9214271. G.J.L. would like to thank the Commission for Educational Exchange between the United States of America, Belgium, and Luxembourg for a Fulbright Research Fellowship during the 1993–1994 academic year. DPM would like to thank the Dutch Foundation of Fundamental Research on Matter for their financial support.

[1] J. F. Herbst, Rev. Mod. Phys. **63**, 819 (1991).
[2] K. H. J. Buschow, Rep. Prog. Phys. **54**, 1123 (1991).
[3] W. B. Yelon, H. Xie, G. J. Long, O. A. Pringle, F. Grandjean, and K. H. J. Buschow, J. Appl. Phys. **73**, 6029 (1993).
[4] G. J. Long, G. K. Marasinghe, S. Mishra, O. A. Pringle, F. Grandjean, K. H. J. Buschow, W. B. Yelon, F. Pourarian, and O. Isnard, Solid State Commun. **88**, 761 (1993).
[5] R. M. Ibberson, O. Moze, T. H. Jacobs, and K. H. J. Buschow, J. Phys.: Condens. Matter **3**, 1219 (1991); W. Steiner and R. Haferl, Phys. Status Solidi A **42**, 739 (1977).
[6] G. J. Long and F. Grandjean, in *Supermagnets, Hard Magnetic Materials*, edited by G. J. Long and F. Grandjean (Kluwer, Dordrecht, 1991), p. 355.
[7] G. J. Long, O. A. Pringle, F. Grandjean, W. B. Yelon, and K. H. J. Buschow, J. Appl. Phys. **74**, 504 (1993).
[8] J. F. Herbst, J. J. Croat, R. W. Lee, and W. B. Yelon, J. Appl. Phys. **53**, 250 (1982).
[9] S. Miraglia, J. L. Soubeyroux, C. Kolbeck, O. Isnard, and D. Fruchart, J. Less-Common Met. **171**, 51 (1991).
[10] T. H. Jacobs, Ph.D. thesis, Leiden University, Leiden, The Netherlands, 1992.
[11] K. H. J. Buschow, Rep. Prog. Phys. **40**, 1179 (1977).
[12] J. M. D. Coey, H. Sun, and Y. Otani, in *Proceedings of the 11th International Workshop on Rare-earth Magnets and their Applications*, Volume II Symposium, edited by S. G. Sankar (Carnegie Mellon University, 1990), p. 36.
[13] G. J. Long, O. A. Pringle, F. Grandjean, and K. H. J. Buschow, J. Appl. Phys. **72**, 4845 (1992).
[14] L. Gelato, J. Appl. Cryst. **14**, 141 (1981).
[15] G. J. Long, G. K. Marasinghe, S. Mishra, O. A. Pringle, Z. Hu, W. B. Yelon, D. P. Middleton, K. H. J. Buschow, and F. Grandjean (unpublished).
[16] G. J. Long, S. Mishra, O. A. Pringle, F. Grandjean, and K. H. J. Buschow, J. Appl. Phys. **75**, 5994 (1994).
[17] G. J. Long, O. A. Pringle, F. Grandjean, and K. H. J. Buschow, J. Appl. Phys. **75**, 2598 (1994).
[18] D. L. Williamson, in *Mössbauer Effect Isomer Shifts*, edited by G. K. Shenoy and F. E. Wagner (North Holland, Amsterdam, 1978), p. 317.
[19] A. M. van der Kraan and K. H. J. Buschow, Physica **138B**, 55 (1986).

[20] J. W. C. de Vries, R. C. Thiel, and K. H. J. Buschow, J. Phys. F **15**, 2403 (1985).
[21] C. Rudowics, J. Phys. C **18**, 1415 (1985).
[22] R. Coehoorn and K. H. J. Buschow, J. Appl. Phys. **69**, 5590 (1991).
[23] R. Coehoorn, in *Supermagnets, Hard Magnetic Materials*, edited by G. J. Long and F. Grandjean (Kluwer, Dordrecht, 1991), p. 133.
[24] F. M. Mulder, R. C. Thiel, and K. H. J. Buschow, J. Alloys Compounds **190**, 77 (1992).